Inorg. Chem. **2007**, *46*, 4212–4219

Comparative Study of Uranyl(VI) and -(V) Carbonato Complexes in an Aqueous Solution

Atsushi Ikeda,*,† Christoph Hennig,† Satoru Tsushima,† Koichiro Takao,‡ Yasuhisa Ikeda,‡ Andreas C. Scheinost,† and Gert Bernhard†

Forschungszentrum Dresden-Rossendorf (FZD), Institute of Radiochemistry, P.O. Box 510119, 01314 Dresden, Germany, and Research Laboratory for Nuclear Reactors, Tokyo Institute of Technology, 2-12-1-N1-34 Ookayama, Meguro-ku, Tokyo 152-8550, Japan

Received January 11, 2007

Electrochemical, complexation, and electronic properties of uranyl(VI) and -(V) carbonato complexes in an aqueous Na_2CO_3 solution have been investigated to define the appropriate conditions for preparing pure uranyl(V) samples and to understand the difference in coordination character between UO_2^{2+} and UO_2^{+}. Cyclic voltammetry using three different working electrodes of platinum, gold, and glassy carbon has suggested that the electrochemical reaction of uranyl(VI) carbonate species proceeds quasi-reversibly. Electrolysis of UO_2^{2+} has been performed in Na_2CO_3 solutions of more than 0.8 M with a limited pH range of $11.7 < pH < 12.0$ using a platinum mesh electrode. It produces a high purity of the uranyl(V) carbonate solution, which has been confirmed to be stable for at least 2 weeks in a sealed glass cuvette. Extended X-ray absorption fine structure (EXAFS) measurements revealed the structural arrangement of uranyl(VI) and -(V) tricarbonato complexes, $[UO_2(CO_3)_3]^{n-}$ [$n = 4$ for uranyl(VI), 5 for uranyl(V)]. The bond distances of $U–O_{ax}$, $U–O_{eq}$, U–C, and $U–O_{dist}$ are determined to be 1.81, 2.44, 2.92, and 4.17 Å for the uranyl(VI) complex and 1.91, 2.50, 2.93, and 4.23 Å for the uranyl(V) complex, respectively. The validity of the structural parameters obtained from EXAFS has been supported by quantum chemical calculations for the uranyl(VI) complex. The uranium L_I- and L_{III}-edge X-ray absorption near-edge structure spectra have been interpreted in terms of electron transitions and multiple-scattering features.

Introduction

The assessment of the environmental impact on the geological disposal of radioactive wastes requires vast information about the speciation of radioactive nuclides in order to estimate the migration behavior of nuclides leaked out from underground waste repository sites. Above all, carbonato complexes of actinides are some of the most significant species to be understood because some actinide nuclides have extremely long-lived radiotoxicity and are expected to form various types of complexes with carbonate ions (CO_3^{2-}), which exist plentifully in groundwater, during their long-term transport in the geosphere. Furthermore, carbonate ions are known to form strong complexes with actinides, and their resulting complexes show high mobility due to their high solubility. In fact, extensive studies have already been carried out for actinide carbonates in the last decades.[1]

The carbonato complex of uranium is one of the most essential species not only for the migration study on radioactive waste repositories but also for investigation of the remediation of closed uranium mining. It is well-known that uranium has various oxidation states (i.e., III−VI) and the transport behavior of uranium in groundwater strongly depends on its oxidation states. However, trivalent and tetravalent uranium carbonato complexes are expected to be insoluble in underground conditions,[2] and hence they are of less importance for the geological assessment. On the other

* To whom correspondence should be addressed. E-mail: a.ikeda@fzd.de.
† Institute of Radiochemistry.
‡ Tokyo Institute of Technology.

(1) (a) Newton, T. W.; Sullivan, J. C. In *Handbook on the Physics and Chemistry of the Actinides*; Freeman, A. J., Keller, C., Eds.; Elsevier Science Publishers BV: Amsterdam, The Netherlands, 1986; Chapter 10, p 387. (b) Clark, D. L.; Hobart, D. E.; Neu, M. P. *Chem. Rev.* **1995**, *95*, 25−48.

(2) (a) Ciavatta, L.; Ferri, D.; Grenthe, I.; Salvatore, F.; Spahiu, K. *Inorg. Chem.* **1983**, *22*, 2088−2092. (b) Grenthe, I.; Fuger, J.; Konings, R. J. M.; Lemire, R. J.; Muller, A. B.; Nguyen-Trung, C.; Wanner, H. In *Chemical Thermodynamics of Uranium*; Wanner, H., Forest, I., Eds.; OECD-NEA: Paris, 1991; Chapter V, p 308 (2003 updated).

10.1021/ic070051y CCC: $37.00
Published on Web 04/07/2007

hand, hexavalent uranium (i.e., uranyl ions) forms soluble carbonate species in groundwater, being matters of importance. Although pentavalent uranium is unstable in an aqueous solution without a high carbonate content, its importance in the uranyl(VI)/uranyl(IV) redox reaction catalyzed by mineral surfaces has recently been discussed by several researchers.[3]

To date, carbonato complexes of hexavalent uranium (i.e., uranyl(VI) ion, UO_2^{2+}) in an aqueous solution have been well investigated stoichiometrically,[4,5] spectroscopically (UV−visible absorption,[6−8] Raman,[9−11] NMR,[5,11−13] X-ray diffraction,[11,13] and X-ray absorption),[11,14] and theoretically.[15−17] In contrast, there is much less information available on pentavalent uranium (i.e., uranyl(V) ion, UO_2^+) carbonato complexes because UO_2^+ is unstable because of its disproportionation reaction: $2UO_2^+ \rightarrow UO_2\downarrow + UO_2^{2+}$.[18] Although it has already been known that the uranyl(V) carbonato complex can be prepared in an aqueous solution electrochemically[6,7,19] and its fundamental properties have been studied by UV−visible absorption,[6−8] Raman,[10] X-ray absorption,[14] and NMR[19] measurements and theoretical calculation,[16] there are still many aspects to be investigated about the chemistry of the uranyl(V) carbonato complex. For instance, the extended X-ray absorption fine structure (EXAFS) study by Docrat et al.[14] is the only available information about the structure of the uranyl(V) carbonato complex in an aqueous solution so far. They succeeded in determining the local arrangement [i.e., coordination numbers (*N*) and bond distances (*R*)] of the uranyl(V) carbonato complex, revealing that the carbonato complex of the uranyl(V) ion is identical with that of the uranyl(VI) ion and is found to be a tricarbonato complex, $[UO_2(CO_3)_3]^{n-}$ ($n = 5$ for uranyl(V) and 4 for uranyl(VI)). However, this pioneer work unfortunately gave little information on their outer coordination spheres, such as the tilt angle of the carbonate ions (CO_3^{2-}) toward the uranyl center. Furthermore, the structural parameters obtained in this study contained relatively large errors, giving rise to a difficulty in evaluating the validity of related theoretical calculations. In this paper, we investigate the electrochemical and complexation properties of uranyl(V) and -(VI) carbonato complexes by cyclic voltammetry (CV), bulk electrolysis, and X-ray absorption spectroscopy (XAS) combined with density functional theory (DFT) calculations in order to acquire detailed knowledge of uranyl(VI) and -(V) carbonato complexes.

Experimental Section

Materials. As a starting material for all experiments, $Na_4[UO_2(CO_3)_3]$ was synthesized according to the procedure reported previously.[20] This uranyl carbonate compound was dissolved in a desired concentration of an aqueous Na_2CO_3 solution to give a concentration of 50 mM UO_2^{2+} and used both for electrochemical experiments and for XAS measurements. All of the chemicals [except $UO_2(NO_3)_2 \cdot 6H_2O$, supplied by Lachema Ltd.] used in this study are reagent grade and supplied by Wako Pure Chemical Industries, Ltd., and Merck KGaA.

Electrochemical Experiments. Cyclic voltammograms of a uranyl carbonate solution (50 mM UO_2^{2+} in a 1.0 M Na_2CO_3 solution) were recorded at 278 K with a Bioanalytical System Inc. (BAS) CV-50W voltammetric analyzer under a dry argon atmosphere by using a three-electrode system: a platinum wire counter electrode, a Ag/AgCl reference electrode, and three different working electrodes (platinum, gold, and glassy carbon). The surface areas of the working electrodes were 2.01 mm^2 for the platinum and gold electrodes and 7.07 mm^2 for the glassy carbon electrode. Sample solutions for CV were deoxygenated by bubbling dry argon gas into the solutions for at least 3 h in advance. CV of a blank 1.0 M Na_2CO_3 solution was also performed for each working electrode so that we could exclude the influence of the non-faradaic current, such as the charging current or liquid junction potential. The cyclic voltammograms of the blank solution are given in the Supporting Information. For preparing the uranyl(V) samples for XAS measurements, bulk electrolysis of the uranyl(VI) carbonate solution was performed at a constant reduction potential of −900 mV (vs Ag/AgCl), controlled by a Meinsberger potentiostat/galvanostat PS6, under dry

(3) (a) Privalov, T.; Schimmelpfennig, B.; Wahlgren, U.; Grenthe, I. *J. Phys. Chem. A* **2003**, *107*, 587−592. (b) Ilton, E. S.; Haiduc, A.; Cahill, C. L.; Felmy, A. R. *Inorg. Chem.* **2005**, *44*, 2986−2988. (c) Wander, M. C. W.; Kerisit, S.; Rosso, K. M.; Schoonen, M. A. A. *J. Phys. Chem. A* **2006**, *110*, 9691−9701.
(4) (a) Blake, C. A.; Coleman, C. F.; Brown, K. B.; Hill, D. G.; Lowrie, R. S.; Schmitt, J. M. *J. Am. Chem. Soc.* **1956**, *78*, 5978−5983. (b) Cinnéide, S. Ó.; Scanlan, J. P.; Hynes, M. J. *J. Inorg. Nucl. Chem.* **1975**, *37*, 1013−1018. (c) Scanlan, J. P. *J. Inorg. Nucl. Chem.* **1977**, *39*, 635−639. (d) Ciavatta, L.; Ferri, D.; Grimaldi, M.; Palombari, R.; Salvatore, F. *J. Inorg. Nucl. Chem.* **1979**, *41*, 1175−1182. (e) Maya, L. *Inorg. Chem.* **1982**, *21*, 2895−2898. (f) Grenthe, I.; Ferri, D.; Salvatore, F.; Riccio, G. *J. Chem. Soc., Dalton Trans.* **1984**, 2439−2443.
(5) Ciavatta, L.; Ferri, D.; Grenthe, I.; Salvatore, F. *Inorg. Chem.* **1981**, *20*, 463−467.
(6) Cohen, D. *J. Inorg. Nucl. Chem.* **1970**, *32*, 3525−3530.
(7) Wester, D. W.; Sullivan, J. C. *Inorg. Chem.* **1980**, *19*, 2838−2840.
(8) (a) Mizuguchi, K.; Park, Y.-Y.; Tomiyasu, H.; Ikeda, Y. *J. Nucl. Sci. Technol.* **1993**, *30*, 542−548. (b) Mizuoka, K.; Tsushima, S.; Hasegawa, M.; Hoshi, T.; Ikeda, Y. *Inorg. Chem.* **2005**, *44*, 6211−6218.
(9) Maya, L.; Begun, G. M. *J. Inorg. Nucl. Chem.* **1981**, *43*, 2827−2832.
(10) Madic, C.; Hobart, D. E.; Begun, G. M. *Inorg. Chem.* **1983**, *22*, 1494−1503.
(11) Allen, P. G.; Bucher, J. J.; Clark, D. L.; Edelstein, N. M.; Ekberg, S. A.; Gohdes, J. W.; Hudson, E. A.; Kaltsoyannis, N.; Lukens, W. W.; Neu, M. P.; Palmer, P. D.; Reich, T.; Shuh, D. K.; Tait, C. D.; Zwick, B. D. *Inorg. Chem.* **1995**, *34*, 4797−4807.
(12) (a) Strom, E. T.; Woessner, D. E.; Smith, W. B. *J. Am. Chem. Soc.* **1981**, *103*, 1255−1256. (b) Ferri, D.; Glaser, J.; Grenthe, I. *Inorg. Chim. Acta* **1988**, *148*, 133−134. (c) Brücher, E.; Glaser, J.; Toth, I. *Inorg. Chem.* **1991**, *30*, 2239−2241. (d) Bányai, I.; Glaser, J.; Micskei, K.; Tóth, I.; Zékány, L. *Inorg. Chem.* **1995**, *34*, 3785−3796.
(13) Åberg, M.; Ferri, D.; Glaser, J.; Grenthe, I. *Inorg. Chem.* **1983**, *22*, 3981−3985.
(14) Docrat, T. I.; Mosselmans, J. F. W.; Charnock, J. M.; Whiteley, M. W.; Collison, D.; Livens, F. R.; Jones, C.; Edmiston, M. J. *Inorg. Chem.* **1999**, *38*, 1879−1882.
(15) (a) Pyykkö, P.; Li, J.; Runeberg, N. *J. Phys. Chem.* **1994**, *98*, 4809−4813. (b) Hemmingsen, L.; Amara, P.; Ansoborlo, E.; Field, M. J. *J. Phys. Chem.* **2000**, *104*, 4095−4101. (c) Majumdar, D.; Roszak, S.; Balasubramanian, K.; Nitsche, H. *Chem. Phys. Lett.* **2003**, *372*, 232−241.
(16) Gagliardi, L.; Grenthe, I.; Roos, B. O. *Inorg. Chem.* **2001**, *40*, 2976−2978.
(17) Tsushima, S.; Uchida, Y.; Reich, T. *Chem. Phys. Lett.* **2002**, *357*, 73−77.
(18) Kern, D. M. H.; Orlemann, E. F. *J. Am. Chem. Soc.* **1949**, *71*, 2102−2106.
(19) Mizuoka, K.; Grenthe, I.; Ikeda, Y. *Inorg. Chem.* **2005**, *44*, 4472−4474.
(20) Academy of Sciences of The U.S.S.R., Institute of General and Inorganic Chemistry im N. S. Kurnakov. In *Complex Compounds of Uranium*; Chernyaev, I. I., Ed.; Israel Program for Scientific Translations: Jerusalem, Israel, 1966; Chapter 2, p 34.

Table 1. Redox Parameters for the Uranyl(VI)/Uranyl(V) Couple Estimated from CV

working electrode	diffusion coefficient for oxidized species $(D_O)/(cm^2/s)^c$	transfer coefficient (α)	standard rate constant (k^0)/(cm/s) from the $v^{1/2}$ vs Ψ plot	standard rate constant (k^0)/(cm/s) from the $E_p - E^{0\prime}$ vs ln i_{pc} plot
platinum	2.48×10^{-6}	0.593 ± 0.050	$2.36 (\pm 0.35) \times 10^{-4}$	$6.25 (\pm 0.15) \times 10^{-5}$
gold	2.81×10^{-6}	0.364 ± 0.008	$2.39 (\pm 0.21) \times 10^{-4}$	$2.31 (\pm 0.06) \times 10^{-4}$
glassy carbon	3.73×10^{-6}	0.111 ± 0.007	$6.01 (\pm 0.97) \times 10^{-5}$	$5.44 (\pm 0.01) \times 10^{-5}$
mercury[29a]	7.2×10^{-6}	0.41	2.6×10^{-5}	
mercury[32b]	3.6×10^{-6}	0.43−0.45	8.91×10^{-5}	

[a] The values were estimated from the cyclic voltammograms obtained for 10 mM UO_2^{2+} in a 0.1 M Na_2CO_3 solution at pH 11.3. [b] The values were estimated from polarography for 2.0−12.4 mM UO_2^{2+} in a 1.0 M Na_2CO_3 solution. [c] Errors were less than ±2%.

dinitrogen atmosphere using a platinum mesh working electrode [80 mesh, 35 × 25 mm, supplied by BAS], a platinum wire counter electrode, and a Ag/AgCl reference electrode. A Vycor glass diaphragm was employed to separate counter and reference electrodes from the sample solution. After approximately 3 h of electrolysis, the solution became completely colorless as previously reported.[6,7] The electrolysis was performed in an inert gas glovebox (the dioxygen concentration in the glovebox was less than 1 ppm). UV−visible absorption spectra of the sample were collected before and after the electrolysis using a Cary 5G (Varian, Inc.) UV−visible−near-IR spectrophotometer to analyze the species in the sample.

XAS Measurements. XAS measurements (EXAFS and XANES) were carried out on the Rossendorf Beamline BM20[21] at the European Synchrotron Radiation Facility under dedicated ring operating conditions (6.0 GeV; 180−200 mA). A Si(111) double-crystal monochromator was employed in channel-cut mode. Uranium L_I- and L_{III}-edge spectra were collected in transmission mode using argon-filled ionization chambers at ambient temperature and pressure. The energy of the spectra was calibrated by the simultaneous XAS measurement of reference Y foil (first inflection point at 17 038 eV). The threshold energy, E_0, of uranium L_{III} edge was defined as 17 185 eV both for uranyl(V) and for uranyl(VI). The spectra were treated by using the data analysis program WinXAS[22] (version 3.1). Theoretical phase and amplitude functions were calculated from the program FEFF 8.20.[23] The spectra were fitted by five single-scattering (SS) paths of axial oxygen (O_{ax}), equatorial oxygen (O_{eq}), carbon, distal oxygen (O_{dist}), and sodium atoms [i.e., $U-O_{ax}$, $U-O_{eq}(CO_3^{2-})$, U−C, $U-O_{dist}(CO_3^{2-})$, and U−Na] and two multiple-scattering (MS) paths (i.e., $U-O_{ax}-U-O_{ax}$ and $U-C-O_{dist}-C$), which were derived from the crystal structure of $Na_2Ca[UO_2(CO_3)_3]\cdot xH_2O$.[24] For each curve fit, the amplitude reduction factor, S_0^2, was held fixed at 0.9 and the shift in the threshold energy, ΔE_0, was varied as every shell has the same value to reduce the number of free parameters.

The uranyl(V) carbonate species is extremely sensitive to oxygen.[6,7,10] Therefore, the uranyl(V) sample was placed in a glass cuvette with a 1.0 cm optical path length. The cuvette was sealed up by hot melting. A uranyl(VI) carbonate sample was transferred to a polyethylene container (optical path length = 1.3 cm) and sealed by melting.

Quantum Chemical Calculations. All of the quantum chemical calculations were performed at the B3LYP level in an aqueous phase without any symmetry constraint using *Gaussian 03* package programs.[25] Several DFT studies on actinide complexes[26,27] have recently suggested that the use of single-configurational DFT without including spin−orbit effects is sufficient for optimizing the geometry of the complexes. Therefore, the energy-consistent small-core effective core potential and the corresponding basis set suggested by Dolg et al.[28] were used for uranium, sodium, oxygen, and carbon atoms comprising 60, 10, 2, and 2 electrons in the core, respectively. Uranium and oxygen basis sets were supplemented with two g functions and one d function, respectively. All geometry optimization calculations were followed by vibrational frequency calculations to ensure that no imaginary vibrational frequency was present in optimized geometries.

Results and Discussions

CV. The CV method has already been applied to the study of the uranyl carbonato complex by several researchers.[7,14,29] Nevertheless, the redox kinetics for the uranyl(VI)/uranyl(V) couple in an aqueous carbonate solution has not been defined sufficiently yet. Furthermore, these previous studies employed a mercury working electrode, whose use has been recently restricted in many countries because of its toxicity. Hence, we measured cyclic voltammograms of the uranyl(VI)/uranyl(V) couple in an aqueous carbonate solution using platinum, gold, and glassy carbon working electrodes.

The CV measurements were performed in a 1.0 M Na_2CO_3 solution at pH 12.0. The obtained cyclic voltammograms

(21) Matz, W.; Schell, N.; Bernhard, G.; Prokert, F.; Reich, T.; Claussner, J.; Oehme, W.; Schlenk, R.; Dienel, S.; Funke, H.; Eichhorn, F.; Betzl, M.; Pröhl, D.; Strauch, U.; Hüttig, G.; Krug, H.; Neumann, W.; Brendler, V.; Reichel, P.; Denecke, M. A.; Nitsche, H. *J. Synchrotron Radiat.* **1999**, *6*, 1076−1085.

(22) Ressler, T. *J. Synchrotron Radiat.* **1998**, *5*, 118−122.

(23) Ankudinov, A. L.; Ravel, B.; Rehr, J. J.; Conradson, S. D. *Phys. Rev. B* **1998**, *58*, 7565−7576.

(24) Coda, A.; Giusta, A. D.; Tazzoli, V. *Acta Crystallogr.* **1981**, *B37*, 1496−1500.

(25) Frisch, M. J.; Trucks, G. W.; Schlegel, H. B.; Scuseria, G. E.; Robb, M. A.; Cheeseman, J. R.; Montgomery, J. A., Jr.; Vreven, T.; Kudin, K. N.; Burant, J. C.; Millam, J. M.; Iyengar, S. S.; Tomasi, J.; Barone, V.; Mennucci, B.; Cossi, M.; Scalmani, G.; Rega, N.; Petersson, G. A.; Nakatsuji, H.; Hada, M.; Ehara, M.; Toyota, K.; Fukuda, R.; Hasegawa, J.; Ishida, M.; Nakajima, T.; Honda, Y.; Kitao, O.; Nakai, H.; Klene, M.; Li, X.; Knox, J. E.; Hratchian, H. P.; Cross, J. B.; Bakken, V.; Adamo, C.; Jaramillo, J.; Gomperts, R.; Stratmann, R. E.; Yazyev, O.; Austin, A. J.; Cammi, R.; Pomelli, C.; Ochterski, J. W.; Ayala, P. Y.; Morokuma, K.; Voth, G. A.; Salvador, P.; Dannenberg, J. J.; Zakrzewski, V. G.; Dapprich, S.; Daniels, A. D.; Strain, M. C.; Farkas, O.; Malick, D. K.; Rabuck, A. D.; Raghavachari, K.; Foresman, J. B.; Ortiz, J. V.; Cui, Q.; Baboul, A. G.; Clifford, S.; Cioslowski, J.; Stefanov, B. B.; Liu, G.; Liashenko, A.; Piskorz, P.; Komaromi, I.; Martin, R. L.; Fox, D. J.; Keith, T.; Al-Laham, M. A.; Peng, C. Y.; Nanayakkara, A.; Challacombe, M.; Gill, P. M. W.; Johnson, B.; Chen, W.; Wong, M. W.; Gonzalez, C.; Pople, J. A. *Gaussian 03*, revision C.02; Gaussian, Inc.: Wallingford, CT, 2004.

(26) (a) Macak, P.; Fromager, E.; Privalov, T.; Schimmelpfennig, B.; Grenthe, I.; Wahlgren, U. *J. Phys. Chem. A* **2005**, *109*, 4950−4956. (b) Shamov, G. A.; Schreckenbach, G. *J. Phys. Chem. A* **2005**, *109*, 10961−10974.

(27) Tsushima, S.; Wahlgren, U.; Grenthe, I. *J. Phys. Chem. A* **2006**, *110*, 9175−9182.

(28) Dolg, M.; Wedig, U.; Stoll, H.; Preuss, H. *J. Chem. Phys.* **1987**, *86*, 866−872.

(29) Morris, D. E. *Inorg. Chem.* **2002**, *41*, 3542−3547.

are shown in Figure 1. Each cyclic voltammogram shows a clear reduction peak (−950 to −900 mV for platinum and gold electrodes and −1700 to −1500 mV for the glassy carbon electrode) and an oxidation peak (−700 to −400 mV for platinum and gold electrodes and 0−250 mV for the glassy carbon electrode), corresponding to the reduction of $U^{VI}O_2^{2+}$ to $U^{V}O_2^{+}$ and the reoxidation of $U^{V}O_2^{+}$ to $U^{VI}O_2^{2+}$, respectively. The separation between the cathodic (P_C) and anodic (P_A) peaks (ΔE_p) obviously depends on the scan rate (υ) regardless of the type of working electrode and is significantly larger than that expected for a reversible reaction. Table 1 summarizes the uranyl(VI)/uranyl(V) redox parameters estimated from these cyclic voltammograms according to the method described previously[30] (see the Supporting Information). The standard rate constants (k^0) for this redox system were also estimated from the cathodic peak potential (E_{pc}) and peak current (i_{pc}) of the voltammograms by using the following equation for an irreversible system:[31]

$$i_{pc} = (2.27 \times 10^{-4})FAC_O k^0 \exp[-\alpha(F/RT)(E_{pc} - E^{0\prime})]$$

where F, A, C_O, α, R, T, and $E^{0\prime}$ are the Faraday constant, surface area of the working electrode, concentration of the oxidant, transfer coefficient, gas constant, temperature, and formal potential of the electrode, respectively. The detailed procedure for calculating parameters is described in the Supporting Information. Similar diffusion coefficients (D_O) are obtained for the three tested working electrodes because the composition of the sample solution is exactly the same for the whole measurement. These D_O values for the present carbonate system are one figure smaller than those for other reported aqueous solution systems (0.62×10^{-5} in 0.1 M KCl,[33] 1.05×10^{-5} in 0.1 M HNO_3,[34] and 1.80×10^{-5} in 1 M H_3O_4)[35] but similar to those for the uranyl complexes with organic ligands in a nonaqueous solvent system.[30] It should be noted that, among the four listed electrodes, only a platinum electrode exhibits an α value of above 0.5, implying that the redox reaction of the uranyl(VI)/uranyl(V) couple on a platinum electrode is thermodynamically different from those on other electrodes.[36] In fact, the cyclic voltammograms for the gold electrode show two oxidation peaks that indicate the presence of successive reactions. On the other hand, the

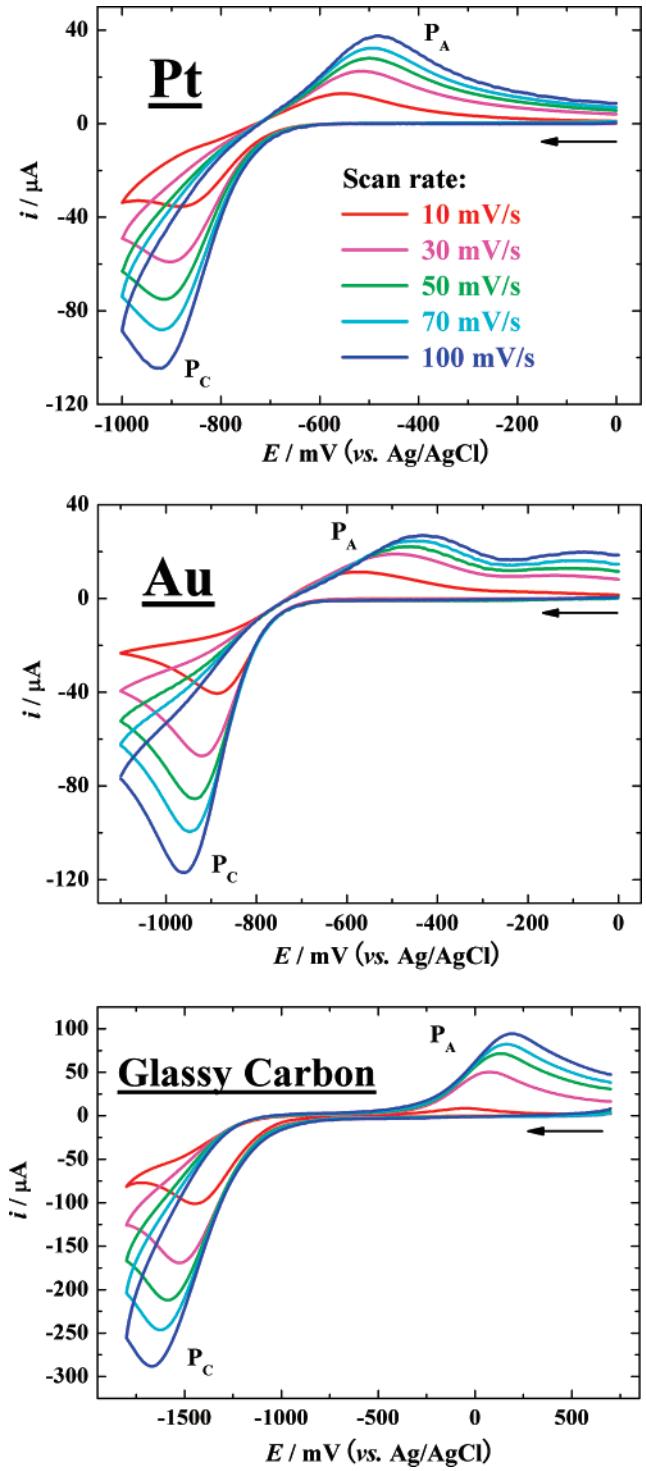

Figure 1. Cyclic voltammograms for 50 mM UO_2^{2+} in a 1.0 M Na_2CO_3 solution (pH = 12.0) using different working electrodes at different scan rates: initial scan direction; cathodic.

k^0 values also give a significant difference among the tested electrodes and increase in the following order: glassy carbon < platinum < gold. This suggests that, from the kinetic point of view, a gold electrode is the most efficient for the larger volume electrolysis to prepare uranyl(V) carbonate samples. However, as mentioned above, the cyclic voltammograms for the gold electrode show two oxidation peaks and, thus, the reduced product on the gold electrode may not be stable because of a successive reaction such as the dissociation of

(30) Mizuoka, K.; Kim, S.-Y.; Hasegawa, M.; Hoshi, T.; Uchiyama, G.; Ikeda, Y. *Inorg. Chem.* **2003**, *42*, 1031−1038.
(31) Bard, A. J.; Faulkner, L. R. *Electrochemical Methods Fundamentals and Applications*, 2nd ed.; John Wiley & Sons: New York, 2001.
(32) Casadio, S.; Orlandini, F. *J. Electroanal. Chem.* **1970**, *26*, 91−96.
(33) Harris, W. E.; Kolthoff, I. M. *J. Am. Chem. Soc.* **1945**, *67*, 1484−1490.
(34) Ghandour, M. A.; Abo-Doma, R. A.; Gomaa, E. A. *Electrochim. Acta* **1982**, *27*, 159−163.
(35) Kacemi, K. E.; Tyburce, B.; Belcadi, S.; Rameau, J. J. *Electrochim. Acta* **1982**, *27*, 729−733.
(36) The transfer coefficient, α, is a measure of the symmetry of the potential energy barrier between reactants and products.[31] Redox reactions can be classified into three systems according to this value; $\alpha = 0.5$, $0 \le \alpha < 0.5$, and $0.5 < \alpha \le 1$. When α equals 0.5, the energy barrier is completely symmetrical. On the other hand, if α is less than 0.5, the energy barrier becomes asymmetrical and the slope of the standard free energy curve for reactants is gentler than that for products. On the contrary, if α is above 0.5, this means that the slope for reactants is steeper than that for products.

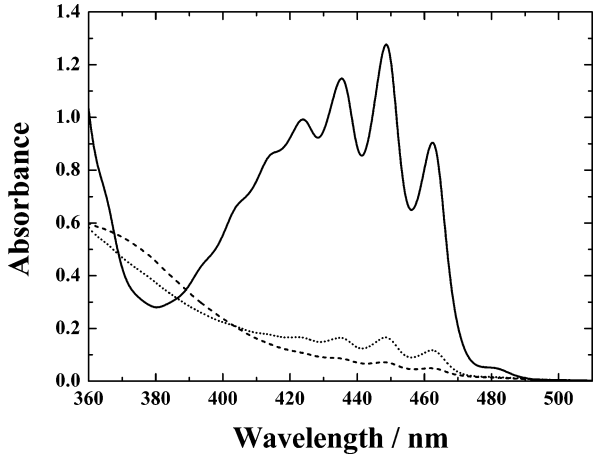

Figure 2. UV−visible absorption spectra for 50 mM UO_2^{2+} in a 1.4 M Na_2CO_3 solution (pH 11.9) before and after electrolysis: solid line, before electrolysis; broken line, immediately after electrolysis and 2 weeks after electrolysis; dotted line, 2 months after electrolysis.

the complex. On the basis of these considerations, we conclude that the platinum electrode is the most appropriate for the efficient bulk electrolysis of uranyl carbonate samples among the three tested electrodes. Accordingly, the following bulk electrolysis was carried out by using the platinum working electrode. Furthermore, in terms of k^0 values, the electrochemical reduction from the uranyl(VI) carbonate species to the uranyl(V) one on the three tested electrodes is categorized as a quasi-reversible system[30,37] and has been interpreted as the electron-transfer limited kinetics.[29]

Bulk Electrolysis. Accurate structural determination of the uranyl(V) carbonato complex by EXAFS requires a pure and stable uranyl(V) sample; otherwise, the observed spectra will be a mixture of uranyl(V) and uranyl(VI) species, and no trustworthy parameters can be obtained. Therefore, a systematic investigation was performed using a platinum mesh electrode in order to reveal the appropriate conditions for stabilizing uranyl(V) species. It was found that the reduced product of the uranyl(V) carbonate species could be stabilized in the Na_2CO_3 solution with concentrations higher than 0.8 M. The electrolysis performed in less than a 0.8 M Na_2CO_3 solution resulted in the production of a fine precipitate with yellow-brown color. Furthermore, the uranyl-(V) carbonate species was stable only in the limited pH range of $11.7 < pH < 12.0$. Any deviation from this pH range gave brownish precipitation, as reported previously.[6,10] Additionally, the stability of the uranyl(V) carbonate species also depended on the concentration of UO_2^{2+}, and it decreased with increasing UO_2^{2+} concentration. On the basis of these results, the uranyl(V) carbonate sample for XAS measurement was prepared in a 1.4 M Na_2CO_3 solution at pH 11.9. The obtained sample solution was completely colorless. Figure 2 shows the UV−visible absorption spectra of the uranyl carbonate solution before and after electrolysis. Characteristic absorption bands for the uranyl(VI) carbonato complex[8] considerably decreased after electrolysis, suggesting that UO_2^{2+} was successfully reduced to UO_2^{+}. The uranyl(V)/uranyl(VI) ratio in the sample after the electrolysis

(37) Matsuda, H.; Ayabe, Y. *Z. Elektrochem.* **1955**, *59*, 494−503.

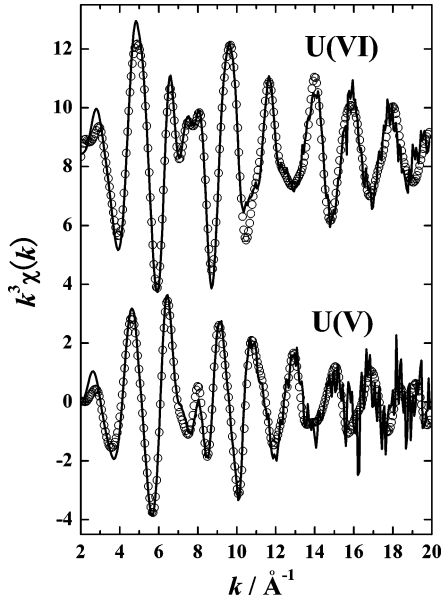

Figure 3. k^3-weighted uranium L_{III}-edge EXAFS spectra for uranyl(VI) and -(V) carbonato complexes in a 1.4 M Na_2CO_3 solution at pH 11.9: −, experimental data; ○, theoretical fit.

was estimated as 94.4/5.6 (M/M) from the absorbances at 447 nm by assuming that the uranyl(V) species has no absorbance at this wavelength.[6,7] The obtained uranyl(V) sample exhibited no spectral change after 2 weeks (i.e., after the XAS measurement), although the absorption bands corresponding to the uranyl(VI) carbonato complex slightly increased after 2 months. Hence, the following XAS results about the uranyl(V) sample can be considered to be attributed only to the uranyl(V) species.

Structural Determination by EXAFS and DFT Calculations. k^3-weighted EXAFS spectra for uranyl(VI) and -(V) carbonato complexes in a 1.4 M Na_2CO_3 solution are shown in Figure 3, and their corresponding Fourier transforms (FTs) are given in Figure 4. Clear EXAFS oscillations were obtained until $k = 20$ Å^{-1} for both uranyl(VI) and uranyl-(V) samples with a sufficient distance resolution ($\Delta R = \pi/2\Delta k$) of 0.09 Å in their FTs. The spectrum for the uranyl-(V) species displays a different oscillation pattern than that of the uranyl(VI) species. On the other hand, their FTs show some similarities concerning the peak arrangement among each other, suggesting that the coordination geometry of the uranyl(VI) and -(V) carbonate complexes remains unchanged. It is clear from the previous reports[11,14,19] that both UO_2^{2+} and UO_2^{+} form a bidentate-coordinated tricarbonato complex, $[UO_2(CO_3)_3]^{n-}$ [$n = 4$ for uranyl(VI) and 5 for uranyl(V)] in a basic Na_2CO_3 solution. Therefore, the coordination numbers (N) were fixed to the tricarbonato complex values in a curve-fitting procedure. The fitting results are given in Table 2. The interatomic distances of the uranyl(VI) complex in the primary coordination sphere, i.e., $U-O_{ax}$ and $U-O_{eq}$, are 1.81 and 2.44 Å, respectively. These bond distances are significantly longer than those in other uranyl(VI) solutions: $R(U-O_{ax})$ and $R(U-O_{eq})$ are 1.75−1.76 and 2.40−2.43 Å in a $HClO_4$ solution[38] and 1.76 and 2.41−2.42 Å in a HCl solution,[39] respectively. The quantum chemical study by Hemmingsen et al.[15b] has suggested that there is a large

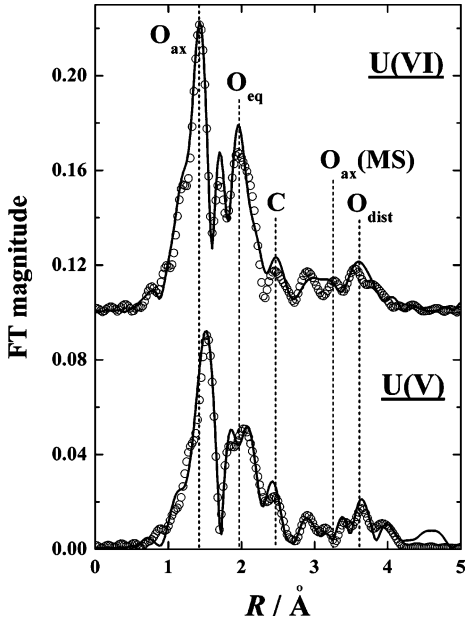

Figure 4. FTs of the EXAFS spectra in Figure 4: —, experimental data; ○, theoretical fit. Phase shifts are not corrected.

Table 2. EXAFS Structural Parameters for Uranyl(VI) and -(V) Carbonato Complexes

	shell	scattering path[a]	N (fixed)	R/Å[b]	σ^2/Å^2 [c]	ΔE_0/eV[d]
uranyl(VI)	O_{ax}	SS	2	1.81	0.0015	5.3
	O_{eq}	SS	6	2.44	0.0059	
	C	SS	3	2.92	0.0030	
	O_{ax}	MS	2	3.60	0.0070	
	O_{dist}	SS	3	4.17	0.0030	
	$C-O_{dist}-C$	MS	3	4.17	0.0039	
uranyl(V)	O_{ax}	SS	2	1.91	0.0023	4.9
	O_{eq}	SS	6	2.50	0.0070	
	C	SS	3	2.93	0.0030	
	O_{ax}	MS	2	3.83	0.0060	
	O_{dist}	SS	3	4.23	0.0030	
	C-O_{dist}-C	MS	3	4.23	0.0030	

[a] SS: single-scattering path. MS: multiple-scattering path. [b] Error: $R \leq \pm 0.01$ Å. [c] Debye−Waller factors. Error: $\sigma^2 \leq \pm 0.0005$ Å^2. [d] Error: $\Delta E_0 \leq \pm 0.1$ eV.

charge transfer from carbonate ions to the uranyl(VI) ion in the uranyl carbonato complex, lengthening the bond distances in the primary coordination sphere. Besides, the bond lengths of U−O_{ax} and U−O_{eq} become 0.10 and 0.06 Å longer as a result of the reduction to uranyl(V), respectively. The uranyl-(VI) tricarbonato complex, $[UO_2(CO_3)_3]^{4-}$, has a closed-shell electronic configuration of $5f^0$. As a result of the reduction from uranyl(VI) to uranyl(V), an additional electron is supposed to enter the $5f_\delta$ or $5f_\phi$ orbital.[40] The DFT calculation in the present study shows that the $[UO_2(CO_3)_3]^{4-}$ complex has four lowest unoccupied molecular orbitals (LUMO to LUMO+3) mainly consisting of U $5f_\delta$ or U $5f_\phi$ atomic orbitals, and they are nearly degenerate. The $[UO_2(CO_3)_3]^{5-}$ complex has the highest occupied molecular orbital (HOMO) composed of the U $5f_\delta$ orbital, and its LUMO to LUMO+2 has U $5f_\delta$ or U $5f_\phi$ characters. The Mulliken population analysis of the uranyl(VI) and -(V) tricarbonato complexes suggests that the net population of U 5f orbitals is 2.49e (σ 1.05, π 0.94, δ 0.11, ϕ 0.39) for uranyl(VI) and 2.72e (σ 0.82, π 0.66, δ 1.04, ϕ 0.20) for uranyl(V). This result indicates that the reduction from uranyl(VI) to uranyl(V) brings an additional electron into the nonbonding U $5f_\delta$ orbital that has little influence on the covalency of bonding. However, this additional electron in the 5f orbital certainly has a screening effect, reducing the effective charge of the uranium atom. This decrease in the effective charge lengthens the U−O_{ax} and U−O_{eq} distances. A similar change in the U−O_{ax} and U−O_{eq} distances has also been observed in a previous theoretical study for uranyl(VI) and -(V) hydrates.[27]

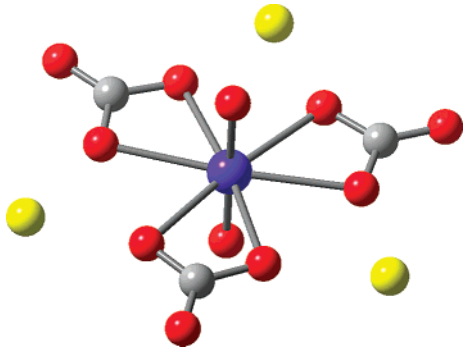

Figure 5. Optimized geometry of the uranyl tricarbonato complex having three sodium ion countercations, $[Na_3UO_2(CO_3)_3]^{n-}$ [$n = 1$ for uranyl(VI) and 2 for uranyl(V)], at the B3LYP level in an aqueous phase.

The $[UO_2(CO_3)_3]^{n-}$ complexes have a high negative charge, and this charge is assumed to be compensated for by countercations.[17,41] Therefore, a curve fit including sodium as the countercation was also performed. This fit yielded a U−Na distance of 3.83 Å for uranyl(VI) and 3.89 Å for uranly(V) and reduced the error of the fit, although this is not certain proof of their presence.

In order to confirm the validity of the structural parameters obtained by EXAFS curve fitting, DFT geometry optimization was performed for both uranyl(VI) and -(V) tricarbonato complexes with and without sodium ion countercation(s). The average interatomic distances obtained from the calculations are summarized in Table 3, and their corresponding structures and the coordinates of the optimized complexes are given in the Supporting Information. For the uranyl(VI) complex, all of the U−O (i.e., U−O_{ax}, U−O_{eq}, and U−O_{dist}) and U−C distances obtained by DFT calculations agree well with the EXAFS results within the difference of 0.02 Å. It was also found that, whereas the geometry of the complexes is distorted when sodium ions are arranged around the complexes, these interatomic distances are hardly affected by the presence of sodium ions and its effect is less than 0.006 Å in U−O and U−C distances. In contrast, there is poor agreement between the calculations and EXAFS results

(38) Sémon, L.; Boehme, C.; Billard, I.; Hennig, C.; Lützenkirchen, K.; Reich, T.; Rossberg, A.; Rossini, I.; Wipff, G. *Chem. Phys. Chem.* **2001**, *2*, 591−598.
(39) Hennig, C.; Tutschku, J.; Rossberg, A.; Bernhard, G.; Scheinost, A. C. *Inorg. Chem.* **2005**, *44*, 6655−6661.
(40) Denning, R. G.; Green, J. C.; Hutchings, T. E.; Dallera, C.; Tagliaferri, A.; Giarda, K.; Brookes, N. B.; Braicovich, L. *J. Chem. Phys.* **2002**, *117*, 8008−8020.
(41) (a) Bernhard, G.; Geipel, G.; Reich, T.; Brendler, V.; Amayri, S.; Nitsche, H. *Radiochim. Acta* **2001**, *89*, 511−518. (b) Majumdar, D.; Balasubramanian, K. *Mol. Phys.* **2005**, *103*, 931−938.

Table 3. Average Interatomic Distances and Vibrational Frequencies of Uranyl(VI) and -(V) Tricarbonato Complexes with and without Na^+ Countercation(s) Optimized at the B3LYP Level

			EXAFS	$[UO_2(CO_3)_3]^{4-}$	$[Na_2UO_2(CO_3)_3]^{2-}$	$[Na_3UO_2(CO_3)_3]^{-}$
uranyl(VI)	*R*/Å	U−O_{ax}	1.81	1.811	1.806	1.805
		U−O_{eq}	2.44	2.461	2.461	2.457
		U−C	2.92	2.925	2.931	2.930
		U−O_{dist}	4.17	4.192	4.191	4.188
		U−Na			3.970	3.961
	vibrational frequency of U−O_{ax}/cm^{-1}	ν_1		810.6	816.6	817.5
		ν_3		853.9	859.3	859.3
			EXAFS	$[UO_2(CO_3)_3]^{5-}$	$[Na_3UO_2(CO_3)_3]^{2-}$	
uranyl(V)	*R*/Å	U−O_{ax}	1.91	1.887	1.881	
		U−O_{eq}	2.50	2.565	2.551	
		U−C	2.93	3.015	3.007	
		U−O_{dist}	4.23	4.298	4.280	
		U−Na			3.935	
	vibrational frequency of U−O_{ax}/cm^{-1}	ν_1		731.3	737.6	
		ν_3		702.2	702.7	

for the uranyl(V) complex. Such a deviation has also been reported at the MBPT2 level calculations.[16] Therefore, the deviation does not arise from the algorithm of DFT itself. Probably we need a more appropriate molecular model for the uranyl(V) complex of $[UO_2(CO_3)_3]^{5-}$, which has a large negative charge, to calculate it correctly. Three sodium ion countercations placed in the equatorial shell (i.e., $[Na_3UO_2(CO_3)_3]^{n-}$, illustrated in Figure 5) eventually shortened the U−O_{eq} distance to 2.54−2.57 Å.

There is also theoretical evidence that the uranyl(V) complex possesses "apical" water molecules on its axial oxygens.[27] The weakening of the U−O_{ax} bond by the reduction from uranyl(VI) to uranyl(V) is expected to make electrons more localized on the axial oxygen atoms. In fact, the effective charge on the axial oxygen is calculated to be −0.50 and −0.75 for uranyl(VI) and uranyl(V), respectively. This larger effective charge on the axial oxygen may enable the formation of hydrogen bonds between the axial oxygen atoms and water molecules.[27] Unfortunately, it is difficult to prove this hypothesis by EXAFS because such apical waters are located too far from the uranium center to detect. However, these apical waters bring a significant electron transfer from uranyl(V) to the apical waters, increasing the effective charge of uranium and shortening the U−O_{eq} bond distance. This effect of apical waters may be one of the possible origins of the observed discrepancy between EXAFS and DFT calculations. We have made an attempt to compute the effect of apical waters. However, the calculations have not converged, and no reasonable result has been obtained so far.

Furthermore, the present study succeeded in obtaining detailed structural information about the outer coordination sphere. The U−C distance for the uranyl(V) complex is almost identical with that for the uranyl(VI) one despite the above-mentioned 0.06 Å difference in the U−O_{eq} distance, indicating that the bending angle of the carbonate ion, O_{eq}−C−O_{eq}, increases from 111° to 116° as the uranyl center is reduced from UO_2^{2+} to UO_2^{+} (see the Supporting Information). This may arise from weakening of the bond strength between U and O_{eq} due to a decrease in the positive charge of the uranyl center. Two significant four-legged MS paths of U−O_{ax}−U−O_{ax}−U and U−C−O_{dist}−C−U were also observed at appropriate distances.[42]

Characterization of XANES. Uranium L_I- and L_{III}-edge XANES spectra for uranyl(VI) and -(V) tricarbonato complexes are shown in Figure 6. The experimental edge energy, which was taken as the first maximum of the first derivative of the spectra, is given in Table 4. The fine structure around the absorption edge generally comprises the contribution of the electron transitions into atomlike orbitals and MS features. The L_{III}-edge spectrum (lower graph in Figure 6) shows a strong resonance (P_1), which mainly originates from the dipole-allowed transition of a $2p_{3/2}$ electron to the final 6d state. An additional transition into the 8s state is of minor importance. In contrast, the L_I-edge spectrum (upper graph in Figure 6) exhibits a weak resonance related with the 2s → 7p transition. The observed shift in the absorption edge position is attributed to the different formal charge of the uranium atom. Several procedures are in use for determining the energy of the absorption edge threshold, E_0.[43] A common reference for the determination of E_0 is the first maximum of the first derivative of the rising edge. In the present study, the reduction from uranyl(VI) to uranyl(V) results in chemical shifts of −0.6 and −2.2 eV at the L_I and L_{III} edges, respectively. However, this approximation of E_0 is ambiguous because the edge position is on the superposition of discrete resonances. On the other hand, the MS paths in the XANES region of uranyl(VI) have been assigned by Templeton and Templeton[44] and Hudson et al.[45] from polarized XAS measurements. The observed XANES spectra of uranyl(V) are analogous to those of uranyl(VI), permitting application

(42) In principle, the *R* value for the U−O_{ax}−U−O_{ax}−U path should be double *R*(U−O_{ax},SS), and the value for the U−C−O_{dist}−C−U path should be equal to *R*(U−O_{dist}). That is, *R*(U−O_{ax},MS) = 2*R*(U−O_{ax},SS) and *R*(C−O_{dist}−C,MS) = *R*(U−O_{dist},SS).

(43) Hennig, C. *Phys. Rev. B* **2007**, *75*, 035120.
(44) Templeton, D. H.; Templeton, L. K. *Acta Crystallogr.* **1982**, *A38*, 62−67.
(45) Hudson, E. A.; Allen, P. G.; Terminello, L. J.; Denecke, M. A.; Reich, T. *Phys. Rev. B* **1996**, *54*, 156−165.

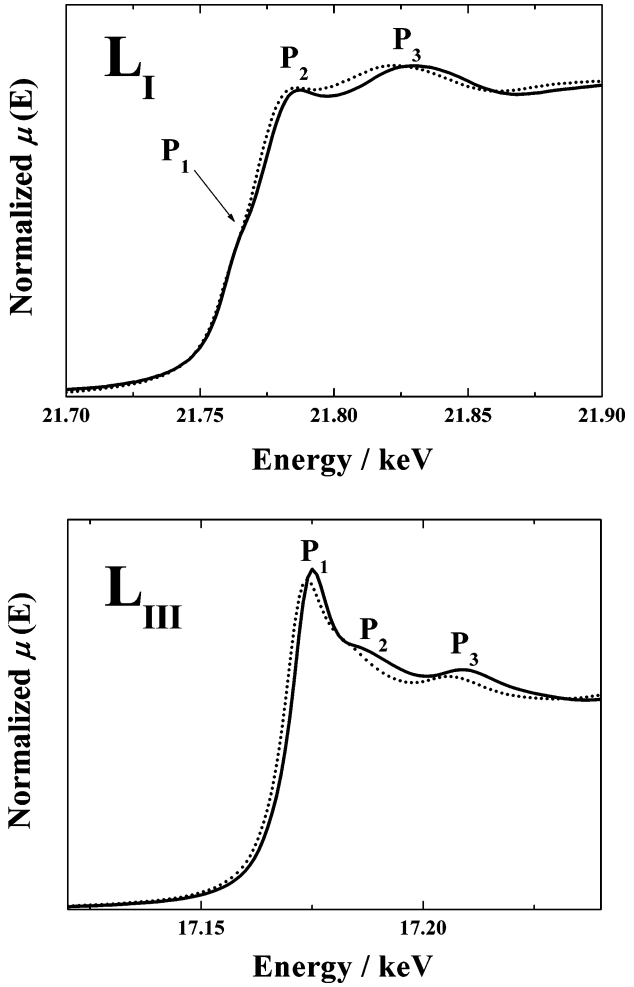

Figure 6. Uranium L_I- (upper) and L_{III}-edge (lower) XANES spectra for uranyl(VI) and -(V) tricarbonato complexes: solid line, the uranyl(VI) complex; dotted line, the uranyl(V) complex.

Table 4. Summary of XANES Spectra for Uranyl(VI) and -(V) Tricarbonato Complexes[a]

		absorption edge/eV	P_2/eV	P_3/eV
L_I	uranyl(VI)	21761.1	21787.4	21830.0
	uranyl(V)	21760.5	21786.1	21822.0
L_{III}	uranyl(VI)	17173.3	17175.2	17208.8
	uranyl(V)	17171.1	17173.9	17205.7

[a] All values were taken as the maximum of the first derivative of each peak. The energies of the absorption edges are not identical with those of the P_1 peaks.

of the above assignment of MS paths for uranyl(VI) to those for uranyl(V) as well. The peaks P_1 at the L_I edge and P_2 at the L_{III} edge originate in the MS of axial oxygen atoms, while the peaks P_2 at the L_I edge and P_3 at the L_{III} edge arise from the MS of equatorial oxygen atoms or more distant atoms. In general, the MS peaks of uranyl(V) spectra are observed at lower energy than those of uranyl(VI). The positions of these MS peaks are closely related with the bond lengths R, that is, $1/R^2$ is in proportion to ΔE, the difference between the MS resonance and the average potential of the interstitial region, V_0.[46] It is noteworthy that the MS feature of $U-O_{ax}$ in the L_{III}-edge spectrum of uranyl(V) is hidden by the strong resonance of the $2p_{3/2} \rightarrow 6d$ transition owing to the above-mentioned energy shift of the edge position. A similar phenomenon was also observed at the protactinium L_{III} edge,[47] where the MS feature of $Pa-O_{ax}$ [$R(Pa-O) = 1.72$ Å] is superposed on the $2p_{3/2} \rightarrow 6d$ transition.

Conclusions

A detailed data analysis of CV suggests that the electrochemical reaction of UO_2^{2+} using platinum, gold, and glassy carbon electrodes in an aqueous Na_2CO_3 solution produces UO_2^{+} quasi-reversibly, and a platinum electrode is the most appropriate working electrode for efficient bulk electrolysis to prepare uranyl(V) carbonate samples among the three tested electrodes. The uranyl(V) carbonate species is stable in a Na_2CO_3 concentration higher than 0.8 M with the limited pH range of $11.7 < pH < 12.0$. A comparison of the structural parameters obtained by EXAFS with quantum chemical calculation results reveals the structural arrangement of uranyl(VI) and -(V) tricarbonato complexes. The reduction from uranyl(VI) to uranyl(V) lengthens all of the bond lengths of the complex mainly because of a decrease in the effective charge of the uranium atom because the reduction follows no conformational change in the complex. The XANES spectra of both uranyl(VI) and -(V) tricarbonato complexes are interpreted by the combination of electron transitions and MS features.

Acknowledgment. This work was supported by the Deutsche Forschungsgemeinschaft under Contract HE 2297/2-1. All of the DFT calculations were performed at Zentrum für Informationsdienste und Hochleistungsrechnen (ZIH), Technische Universität Dresden, Germany. We are thankful for its generous allocation of computational time on the SGI Altix 3700 supercomputer. S.T. was supported by the research fellowship of the Alexander von Humboldt Foundation.

Supporting Information Available: CV data of blank solutions, calculation details, tables of electrochemical data, structures, IR spectra, and coordinates calculated from DFT. This material is available free of charge via the Internet at http://pubs.acs.org.

IC070051Y

(46) (a) Nakamatsu, H. *Chem. Phys.* **1995**, *200*, 49−62. (b) Denecke, M. A. In *Proceedings of the Workshop on Speciation, Techniques and Facilities for Radioactive Materials at Synchrotron Light Sources*; OECD−NEA: Paris, 1999; pp 135−141.

(47) Le Naour, C.; Trubert, D.; Di Giandomenico, M. V.; Fillaux, C.; Den Auwer, C.; Moisy, P.; Hennig, C. *Inorg. Chem.* **2005**, *44*, 9542−6546.